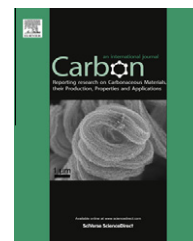


Available at www.sciencedirect.com

SciVerse ScienceDirect

journal homepage: www.elsevier.com/locate/carbon

Passivation of microbial corrosion using a graphene coating

A. Krishnamurthy ^{a,1}, V. Gadhamshetty ^{b,*}, R. Mukherjee ^a, Z. Chen ^c, W. Ren ^c,
H-M. Cheng ^c, N. Koratkar ^{a,*}

^a Mechanical, Aerospace and Nuclear Engineering, Rensselaer Polytechnic Institute, 110 8th Street, Troy, NY 12180, USA

^b Civil and Environmental Engineering, Rensselaer Polytechnic Institute, 110 8th Street, Troy, NY 12180, USA

^c Shenyang National Laboratory for Materials Science, Institute of Metal Research, Chinese Academy of Sciences, Shenyang 110016, China

ARTICLE INFO

Article history:

Received 21 November 2012

Accepted 18 December 2012

Available online 5 January 2013

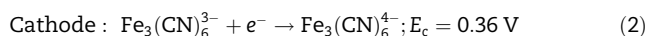
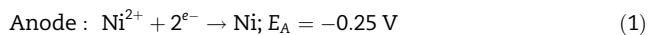
ABSTRACT

Microbial corrosion limits the use of metallic structures in a variety of technological processes and applications. Here, we report the first demonstration of graphene as a passive layer that retards microbially-induced galvanic corrosion (MIC) of metals for extended periods of time (~2700 h). The effectiveness of the MIC-resistant graphene coating was evaluated under realistic operating conditions by testing baseline Ni foams and graphene-coated Ni foams as anodes in a microbial fuel cell. The rates of Ni dissolution in the graphene-coated Ni anode were at least an order of magnitude lower than the baseline (uncoated) Ni electrode. Electrochemical impedance spectroscopy characterization revealed that the MIC of Ni was impeded by over 40-fold when coated with graphene.

© 2013 Elsevier Ltd. All rights reserved.

1. Introduction

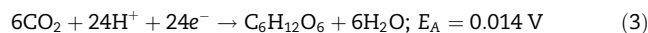
The annual costs related to corrosion have been estimated to be nearly \$276 billion and represents 3.1% of the U.S. Gross Domestic Product [1]. Metallic corrosion is a major contributor to these costs especially in oil production, power plants, shipping and aviation industries, drinking water systems, pipelines, bridges, and public buildings [1,2]. While corrosion typically occurs under acidic conditions, microbial corrosion is more complex as the microbes are adept at inducing corrosion even under ambient temperatures and neutral pH conditions [2]. The galvanic corrosion process can be represented as two half-cell reactions, namely: (i) the oxidation of electron donors (i.e. metals such as Ni) (Eq. (1)) and (ii) the reduction of electron acceptors (Eq. (2)).



In an aqueous environment, microbes develop biofilm layers on the metal surface, and accelerate metallic corrosion by

altering the metal-solution interface [2,3]. Classic techniques to prevent MIC includes physical (e.g. flushing) and chemical methods (e.g. biocides), and by application of passivation layers (e.g. thiol-based mono-layers) [2]. While graphene (Gr) coatings have been reported to be resistant towards oxidation and corrosion in abiotic environments [4–9], there is so far no report on the microbial corrosion resistance of graphene. Here we report that conformal graphene coatings are remarkably effective in inhibiting microbially-induced metallic corrosion (MIC) for time periods of up to 2700 h.

Microbial fuel cells (MFCs) represent a galvanic cell that produces electric current by integrating: (i) bioelectrochemical oxidation of organic matter at the anode (Eq. (3)) and (ii) abiotic reduction of electron acceptor at the cathode (Eq. (2)) [10]



MFCs have been widely used as a galvanic tool to simulate extracellular electron transfer mechanisms of microbes and the bio-electrochemical oxidation of organic matter [10]. Metal anodes are typically not used in MFCs since they are strongly susceptible to galvanic corrosion. In this study, we

* Corresponding author.

E-mail addresses: gadhav@rpi.edu (V. Gadhamshetty), koratn@rpi.edu (N. Koratkar).

¹ These authors contributed equally to this work.

0008-6223/\$ - see front matter © 2013 Elsevier Ltd. All rights reserved.

<http://dx.doi.org/10.1016/j.carbon.2012.12.060>

employ MFCs as a test-bed to study the MIC of nickel-anode (Ni) and graphene-coated-nickel anode (Gr/Ni) in nickel-anode-based MFCs (NABMs), with the objective of demonstrating the MIC resistance of graphene coatings.

2. Experimental procedure

Fig. 1a shows a trimetric view of a two-compartment MFC used in this study. More specifically, three distinct galvanic cells were tested: (i) a Ni-NABM with a Ni anode ($2\text{ cm} \times 2\text{ cm}$), (ii) a Gr-NABM with a Gr/Ni anode ($2\text{ cm} \times 2\text{ cm}$) and (iii) a vitreous carbon (RVC)-MFC with a RVC anode ($2\text{ cm} \times 2\text{ cm}$). The cathode in all the three galvanic cells was a carbon-fiber brush whose surface area was several-fold higher than that of the anode. This ensures that the anode and not the cathode limits the MFC performance. The anode compartment contained mixed microbial populations and glucose-based electrolyte, and the Ni anode ($\text{CO}_2/\text{C}_6\text{H}_{12}\text{O}_6$, $E^0 = -0.36\text{ V}$; Ni^{2+}/Ni , $E^0 = -0.36\text{ V}$) was polarized against a ferricyanide catholyte ($\text{FeCN}_6^{3-}/\text{FeCN}_6^{4-}$; $E^0 = 0.36\text{ V}$) yielding ideal conditions for the galvanic corrosion of Ni in NABMs. The Ni anode in NABMs

was replaced with RVC in the RVC-MFC. The three galvanic cells were operated in a fed-batch mode, and the specific microbial corrosion behavior of the Ni in NABMs was evaluated for extended duration of up to 2700 h.

Nickel was chosen as a model for the metal-based anode in our MIC studies due to its wide-spread relevance in a broad range of industrial applications, and the ease with which Gr could be directly grown over Ni surfaces. A conformal graphene coating was deposited over porous Ni foam (Fig. 1b) via template-directed chemical vapor deposition as described in our previous work [11]. The Raman spectra in Fig. 1c indicates the characteristic G and 2D bands of typical Gr/Ni foam synthesized in our lab. We used the Raman spectra in Fig. 1c to estimate the number of Gr layers in the coating. It is well established that the ratio of the intensity of the Raman 2D peak to G peak can be used to estimate the number of Gr layers in the film [11–12]. In Fig. 1c, the bottom, middle and top spectrum are obtained from different locations on the foam surface. The intensity ratio of the 2D peak to G peak of the bottom, middle and top spectrum are 2.1 (indicative of monolayer), 1.1 (indicative of bi-layer) and 0.68 (indicative of

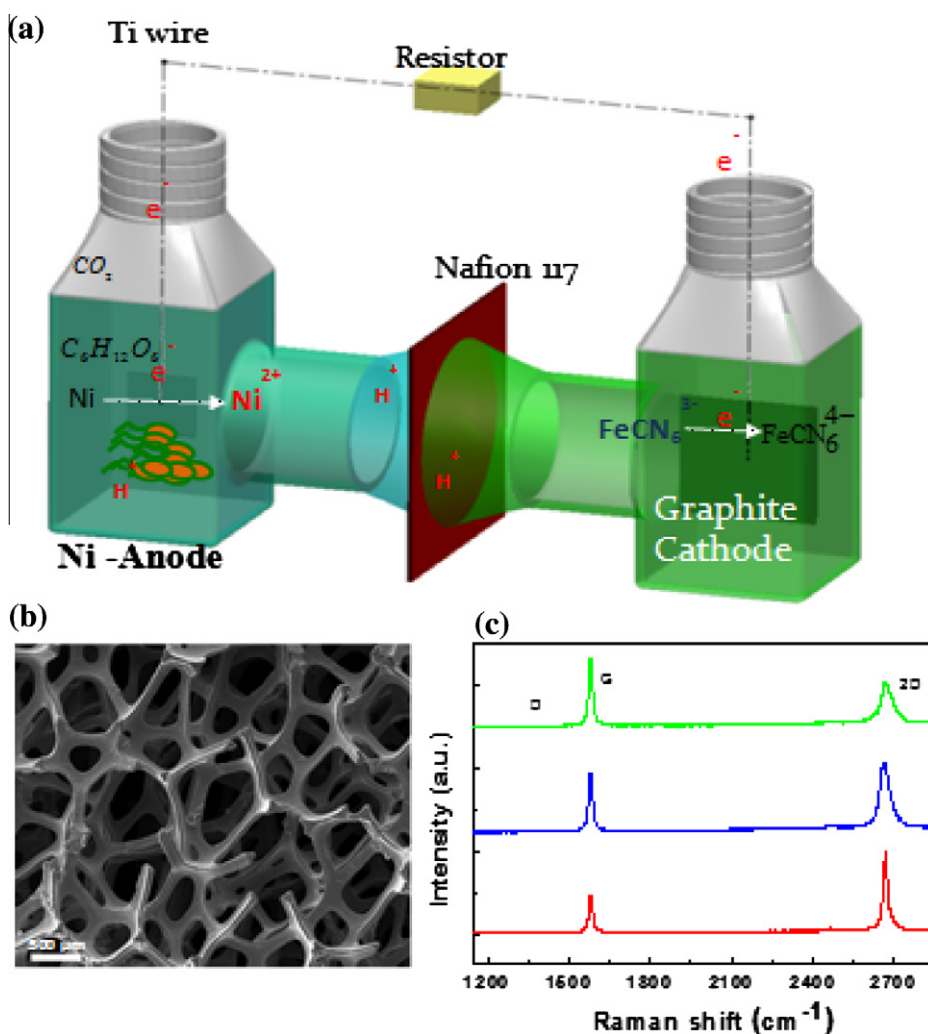


Fig. 1 – (a) Schematic of a galvanic cell used in this study, (b) SEM image of Gr/Ni obtained via chemical vapor deposition and (c) Raman spectra of Gr/Ni electrode. The bottom, middle and top spectrum are obtained from different locations on the foam surface and are indicative of monolayer, bi-layer and tri-layer graphene, respectively [11–12].

tri-layer). Therefore we estimate that the graphene skin is comprised of few-layered (between 1 and 3 layers) graphene sheets. Both Ni and Gr/Ni foams represent 3D micro porous structures with interconnected conductive-scaffolds that are well-suited for microbial growth in an MFC setting.

3. Results and discussion

Fig. 2a–c provides a qualitative, and yet a concrete evidence, for the microbial corrosion of the Ni anode in NABMs. Fig. 2a represents a bare Ni electrode, while Fig. 2b reflects

the fate of the Ni anode in the Ni-NABM after 2000 h of continuous fed-batch operation. Fig. 2b shows the corrosion-induced morphological changes of the Ni electrode, marked with deteriorated edges, significant fractures, and debilitated 3d-scaffolds in the foam structure. The green patches on the Ni foam (Fig. 2b) represents the corrosion products such as Ni(II) compounds. Fig. 2c shows the microbial communities in the biofilm responsible for the MIC of Ni in the Ni-NABM.

The intact structure of a Gr/Ni anode (after ~2800 h of Gr-NABM operation) in Fig. 2d–e is striking and demonstrates the long-term, MIC-resistant properties of the graphene coating.

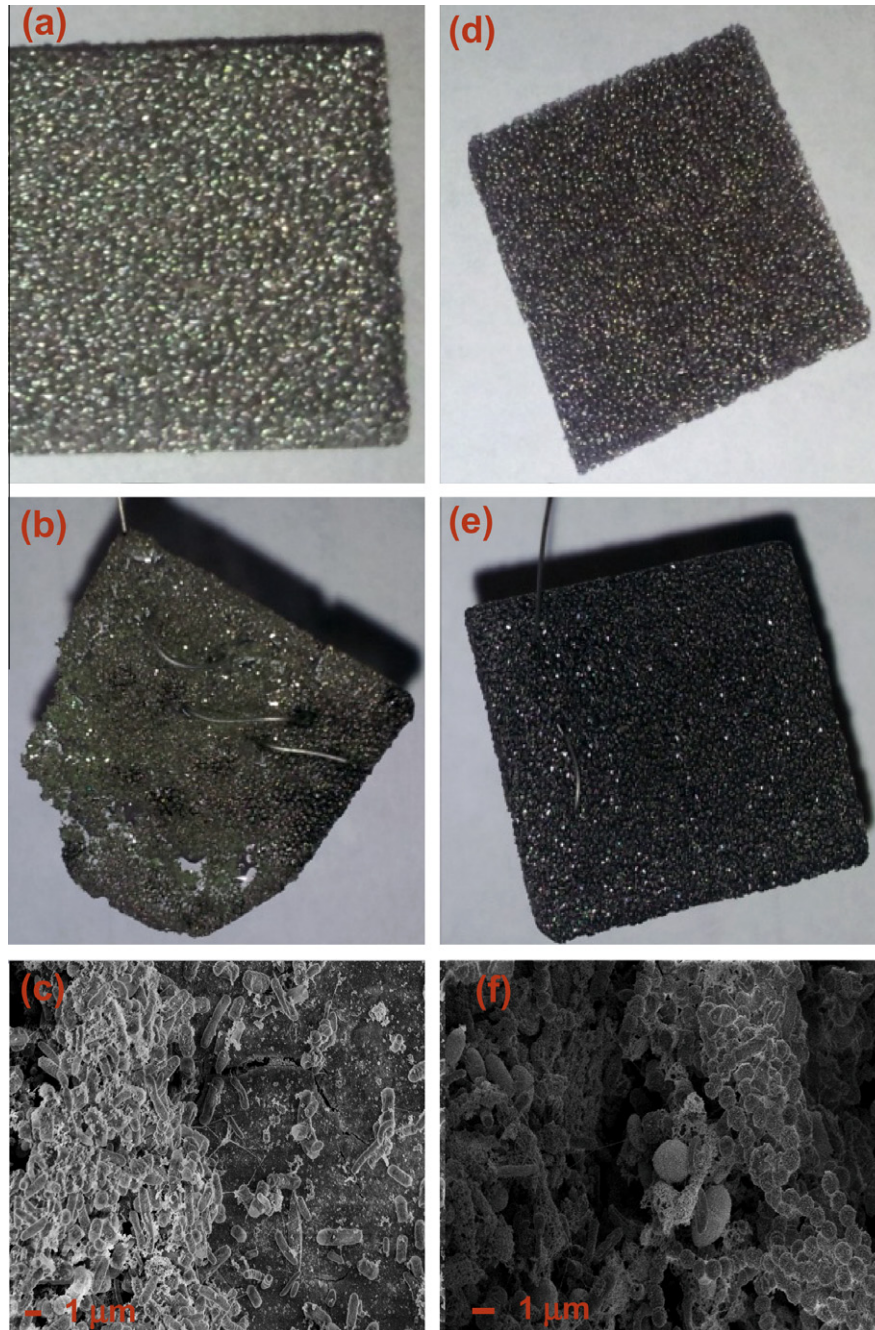


Fig. 2 – (a) A fresh Ni anode, (b) corroded Ni in a Ni-NABM after 2000 h, (c) microbe–Ni interaction on the Ni anode, (d) a fresh Ni/Gr anode, (e) the corrosion resistant Gr/Ni anode in a Gr-NABM after 2800 h and (f) microbial colonies on Gr/Ni surface in the Gr-NABM.

Fig. 2f shows the interconnected microbial network (biofilm) on the Gr/Ni surface due to NABM operation. It should be noted that signs of deterioration on the Ni anode appeared within 10 days, and the Ni electrode has totally collapsed after 80 days of NABM operation; however, the Gr/Ni anode demonstrated excellent anti-MIC properties and retained its physical integrity even after over 110 days of continuous operation (Fig. 2e).

The role of the Gr coating in suppressing Ni corrosion is shown quantitatively in Fig. 3, which shows the instantaneous concentration of Ni in the anolyte throughout the fed-batch operation of the Ni-NABM and Gr-NABM, respectively. The methods used to measure the Ni concentration are described in the Supplementary Information. Note that the galvanic cells were operated in a fed-batch mode, under six consecutive cycles, and in a time span of 2700 h. The transition to the new cycle involved replacement of spent anolyte with equivalent volume of fresh minimal media (Supplementary Information). Each new cycle of the fed-batch operation, involves elimination of planktonic microbes and also Ni in the anolyte. Therefore Fig. 3 does not reflect a temporal trend of Ni accumulation in the galvanic cells; each data point in Fig. 3 is representative of Ni corrosion in a specific cycle of a fed-batch operation. The net accumulation of Ni in each cycle is based on a variety of factors such as biofilm history on the anode; the composition of electrochemically active microbes in the biofilm; the net accumulation of microbial byproducts such as protons, Ni, and organic acids in the biofilm; the anode potential; and the cation transfer capacity of the MFC membrane. Fig. 3 clearly demonstrates the MIC-resistant property of the graphene coating, evident from a significantly lower concentration of soluble Ni in a Gr-NABM as compared to that in a Ni-NABM. In fact, the Gr/Ni anode retained its anti-MIC properties even at $T = 2712$ h of continuous NABM operation, where the soluble Ni in the anolyte of the Gr-NABM was ~ 10 -fold lower than in the Ni-NABM (Fig. 3). The error bars in Fig. 3 represent standard deviation based on average measurement of Ni concentration in three separate tests.

The anodes in NABMs and RVC-MFC were analyzed using Electrochemical Impedance Spectroscopy (EIS) after extended microbial acclimation (>2700 h under 1000Ω). Fig. 4a and b shows a Nyquist plot (Z_{real} vs. $-Z_{\text{img}}$) and a Bode magnitude plot ($|Z|$ vs. ω) for a RVC-MFC, Ni-NABM, and Gr-NABM. The

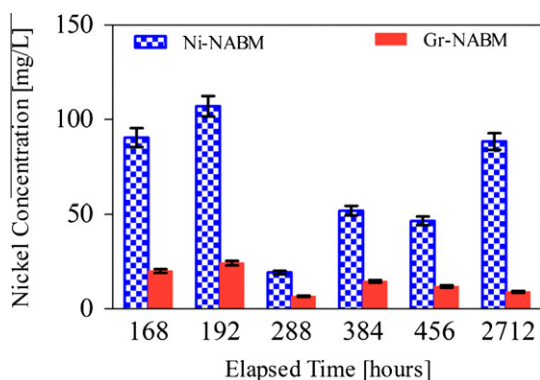


Fig. 3 – Soluble Ni (mg/L) in anolyte of Ni-NABM and Gr-NABM.

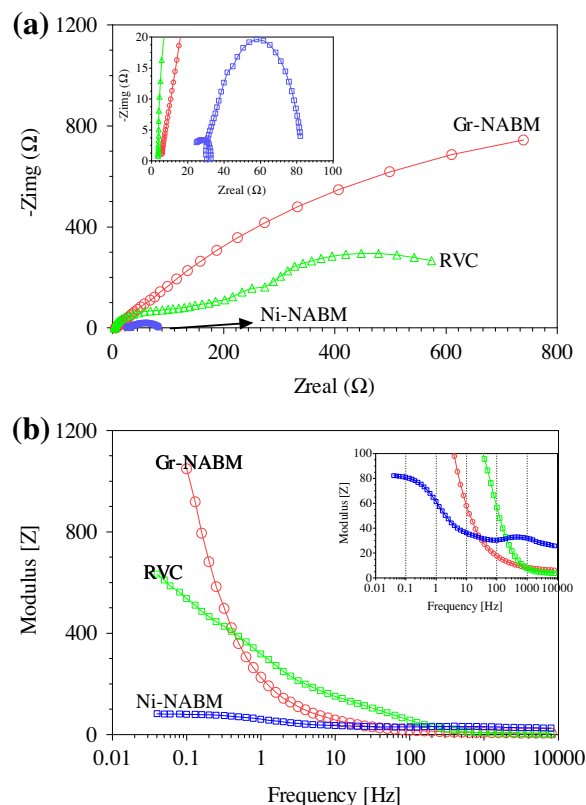


Fig. 4 – EIS analysis of 3 galvanic cells ($T = 2800$ h) (a) Nyquist Plots (b) Bode plots (Insets: clear view of Ni-NABM).

magnitude of the Nyquist arc (i.e. sum of polarization resistance and solution resistance in the low frequency region) qualitatively yields electrochemical polarization (R_p) resistance of the working electrode, and therefore, Fig. 4a demonstrates that R_p offered by Gr/Ni (Gr-NABM) is several orders of magnitude higher than that of Ni (Ni-NABM). Similarly, the Bode plot in Fig. 4b shows that the R_p offered by a Gr-NABM is over 12-fold greater than that in a Ni-NABM. Further, the EIS data were analyzed with electrical equivalent circuit (EEC) fitting method. EEC for a Gr-NABM was modeled as a modified Randles circuit model consisting of an ohmic resistance (R_{el}), a charge transfer resistance between Ni and anolyte (R_{ct}) that accounts for metallic corrosion, a Warburg diffusion element (W), and a constant phase element (CPE) to model the double layer phenomena at the nickel/graphene/anolyte interface (Table S3, Fig. S1 in the Supporting Information).

The EEC for a Ni-NABM was obtained by adding a parallel resistor–capacitor in series (right after R_{el}) to the previously described equivalent circuit in order to account for the microbe-mediated glucose oxidation. Equivalent circuit models and the corresponding fits for each of the three galvanic cells have been provided in the Supplementary section. The excellent corrosion resistance of graphene coating can be inferred by the value of R_{ct} in the Gr-NABM ($35.8 \text{ k}\Omega \text{ cm}^2$) which was ~ 41 -fold higher than in the Ni-NABM ($R_{ct} = 0.86 \text{ k}\Omega \text{ cm}^2$) (Fig. 4a and b).

The curves in Fig. 5 represent cyclic voltammograms (CV) of the Ni, Gr/Ni, and RVC anodes, between -0.6 and 0.8 V at

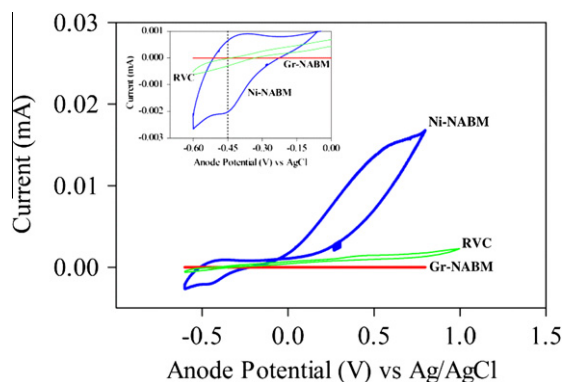


Fig. 5 – Voltammograms in the three galvanic cells ($T = 2800$ h). The inset shows an expanded view of the CV profile in -0.6 – 0 V range.

a scan rate of 5 mV/s. The CV for the Ni-NABM shows distinct oxidation and reduction peaks at -0.45 V (vs. Ag/AgCl^-) which matches with the thermodynamic redox potential of Ni^{2+}/Ni redox couple (Inset in Fig. 5 shows expanded view of CV in the -0.6 – 0 V range). This peak is absent in the RVC-MFC since the Ni anode is replaced by RVC for this case. The absence of Ni/Ni^{2+} redox peak in a Gr-NABM even after 2800 h of MFC operation (Fig. 5) provides compelling evidence of the microbial corrosion resistance of the Gr coating. Another important note is that the range of electrochemical current observed in the CV of the Gr-NABM is over four orders of magnitude lower than that in a Ni-NABM, throughout the entire range of scanned potential values. The RVC data is presented in Figs. 4 and 5 to show that the Gr/Ni response is quite similar to the RVC (pure carbon) electrode even after 2800 h of operation which indicates that the Gr coating is highly successful in shielding the Ni from the microbes and the electrolyte.

4. Summary and conclusions

In summary, this is the first report showing that graphene can inhibit MIC for metal surfaces. Typical passivating agents include inert metals, conductive polymers, and thiol-based monolayers [2]. Such passivating agents can be assembled only on specific metal surfaces and form thicker coatings that alter the physical properties of the underlying metal surface [2,10]. By contrast, graphene is chemically inert and minimally invasive (ultrathin coating). Moreover graphene can be grown on large-area substrates by chemical vapor deposition and can be mechanically transferred onto a range of arbitrary surfaces. Our results indicate that graphene coatings appear to combat MIC by: (i) preventing access of microbes to the Ni surface, (ii) forming a protective barrier between the Ni surface and the anolyte to minimize charge (Ni^{2+}) transport into the solution and (iii) protecting the Ni surface from microbial byproducts (e.g. H^+) that enhance Ni dissolution. For the above functions, the inert graphene coating provides a far

more stable barrier than the oxide films that typically passivate unprotected metal surfaces. Further detailed biochemical investigations are warranted to shed more light on the microbe–graphene and microbe–metal interactions in such systems.

Acknowledgments

N.K. acknowledges support from the Clark and Crossan Endowed Chair Professorship at the Rensselaer Polytechnic Institute. V.G. acknowledges partial funding from NYSPP. H.M.C. acknowledges the funding from NSFC (50921004).

Appendix A. Supplementary data

Supplementary data associated with this article can be found, in the online version, at <http://dx.doi.org/10.1016/j.carbon.2012.12.060>.

REFERENCES

- [1] Koch, G.H., Brongers, P.H., Thompson, N.G., Virmani, Y.P., and Payer, J.H., Corrosion Costs and Prevention Strategies in the United States, Report No. FHWA-RD-01-156, Federal Highway Administration, Washington, DC, March 2002.
- [2] Videla Ha, Herrera LK. Understanding microbial inhibition of corrosion. A comprehensive overview. *Int Biodeterior Biodegradation* 2009;63(7):896–900.
- [3] Little B, Wagner P, Mansfeld F. *Int Mater Rev* 1991;36:253.
- [4] Singh Raman RK, Chakraborty Banerjee P, Lobo DE, Gullapalli H, Sumandasa M, Kumar A, et al. Protecting copper from electrochemical degradation by graphene coating. *Carbon* 2012;50(11):4040–5.
- [5] Prasai D, Tuberquia JC, Harl RR, Jennings GK, Bolotin KI. Graphene: corrosion-inhibiting coating. *ACS Nano* 2012;6(2):1102–8.
- [6] Chen S, Brown L, Levendorf M, Cai W, Ju S-Y, Edgeworth J, et al. Oxidation resistance of graphene-coated Cu and Cu/Ni alloy. *ACS Nano* 2011;5(2):1321–7.
- [7] Chang C-H, Huang T-C, Peng C-W, Yeh T-C, Lu H-I, Hung W-I, et al. Novel anticorrosion coatings prepared from polyaniline/graphene composites. *Carbon* 2012;50(14):5044–51.
- [8] Kirkland NT, Schiller T, Medhekar N, Birbilis N. Exploring graphene as a corrosion protection barrier. *Corros Sci* 2012;56. <http://dx.doi.org/10.1016/j.corsci.2011.12.00>.
- [9] Yua L, Lim YS, Han JH, Kim K, Kim JY, Choi SY, et al. A graphene oxide oxygen barrier film deposited via a self-assembly coating method. *Synth Met* 2012;162(7):710–4.
- [10] Logan BE, Hamelers B, Rozendal R, Schröder U, Keller J, Freguia S, et al. Microbial fuel cells: methodology and technology. *Environ Sci Technol* 2006;40(17):5181–92.
- [11] Chen Z, Ren W, Gao L, Liu B, Pei S, Cheng H-M. Three-dimensional flexible and conductive interconnected graphene networks grown by chemical vapour deposition. *Nat Mater* 2011;10(6):424–8.
- [12] Ferrari AC et al. Raman spectrum of graphene and graphene layers. *Phy Rev Lett* 2006;97:187401.